Journal of Computational Physics 231 (2012) 4515–4529

Contents lists available at SciVerse ScienceDirect

Journal of Computational Physics

journal homepage: www.elsevier.com/locate/jcp

Optimized local basis set for Kohn–Sham density functional theory

Lin Lin [a,*,1], Jianfeng Lu [b], Lexing Ying [c], Weinan E [d,e]

[a] Program in Applied and Computational Mathematics, Princeton University, Princeton, NJ 08544, USA
[b] Courant Institute of Mathematical Sciences, New York University, New York, NY 10012, USA
[c] Department of Mathematics and ICES, University of Texas at Austin, Austin, TX 78712, USA
[d] Department of Mathematics and PACM, Princeton University, Princeton, NJ 08544, USA
[e] Beijing International Center for Mathematical Research, Peking University, Beijing 100871, China

ARTICLE INFO

Article history:
Received 4 August 2011
Received in revised form 10 February 2012
Accepted 13 March 2012
Available online 2 April 2012

Keywords:
Electronic structure
Kohn–Sham density functional theory
Optimized local basis set
Discontinuous Galerkin
Trace minimization
Molecular dynamics
Pulay force
GMRES
Preconditioning

ABSTRACT

We develop a technique for generating a set of optimized local basis functions to solve models in the Kohn–Sham density functional theory for both insulating and metallic systems. The optimized local basis functions are obtained by solving a minimization problem in an admissible set determined by a large number of primitive basis functions. Using the optimized local basis set, the electron energy and the atomic force can be calculated accurately with a small number of basis functions. The Pulay force is systematically controlled and is not required to be calculated, which makes the optimized local basis set an ideal tool for ab initio molecular dynamics and structure optimization. We also propose a preconditioned Newton–GMRES method to obtain the optimized local basis functions in practice. The optimized local basis set is able to achieve high accuracy with a small number of basis functions per atom when applied to a one dimensional model problem.

1. Introduction

In scientific computation of systems with large number of degrees of freedom, an efficient choice of basis functions becomes desirable in order to reduce the computational cost. In this paper, we focus on the choice of efficient basis sets for the Kohn–Sham density functional theory (KSDFT) [1,2], which is the most widely used electronic structure theory for condensed matter systems. The methods and concepts illustrated here are also useful for other applications.

In KSDFT, the quantities of interest are the electron energy $E(R)$ and the atomic force $F(R)$. Here we denote by $R = (R_1, R_2, \ldots, R_{N_A})^T$ the atomic positions, where N_A is the number of atoms. The atomic force is expressed in terms of the derivatives of the electron energy with respect to the atomic positions as $F(R) = -\frac{\partial E(R)}{\partial R}$. This is an important quantity in many applications including structure optimization and first principle molecular dynamics. The electron energy is a functional of a set of Kohn–Sham orbitals $\{\psi_i\}_{i=1}^N$ where N is the number of electrons in the system. To illustrate the idea with minimal technicality, let us consider for the moment a system of non-interacting electrons at zero temperature. The energy functional for non-interacting electrons takes the form

$$E\left(\{\psi_i(x)\}_{i=1}^N; R\right) = \frac{1}{2}\sum_{i=1}^N \int |\nabla\psi_i(x)|^2 \mathrm{d}x + \int V(x;R)\sum_{i=1}^N |\psi_i(x)|^2 \mathrm{d}x. \tag{1}$$

* Corresponding author.
E-mail addresses: linlin@lbl.gov (L. Lin), jianfeng@cims.nyu.edu (J. Lu), lexing@math.utexas.edu (L. Ying), weinan@math.princeton.edu (W. E).
[1] Present address: Computational Research Division, Lawrence Berkeley National Laboratory, Berkeley, CA 94720, USA.

0021-9991/$ - see front matter © 2012 Elsevier Inc. All rights reserved.
http://dx.doi.org/10.1016/j.jcp.2012.03.009

The first term and the second term in (1) are the kinetic energy and the potential energy of the system, respectively. The energy $E(R)$ as a function of atomic positions is given by the following minimization problem

$$\begin{aligned} &E(R) = \min_{\{\psi_i(x)\}_{i=1}^N} E\Big(\{\psi_i(x)\}_{i=1}^N; R\Big), \\ &\text{s.t.} \quad \int \psi_i^*(x)\psi_j(x)\mathrm{d}x = \delta_{ij}, \quad i,j = 1,\ldots,N. \end{aligned} \tag{2}$$

We denote by $\{\psi_i(x;R)\}_{i=1}^N$ the minimizer. It can be readily shown that $\{\psi_i(x;R)\}_{i=1}^N$ are the lowest N eigenfunctions of the Hamiltonian operator $H(R)$, which takes the form

$$H(R) = -\frac{1}{2}\Delta_x + V(x;R). \tag{3}$$

Using the Hamiltonian operator, the electron energy has an alternative expression without the explicit dependence on the orbitals $\{\psi_i\}_{i=1}^N$:

$$E(R) = \mathrm{Tr}[H(R)\chi(H(R) - \mu(R))] \equiv \mathrm{Tr}[g_0(H(R))], \tag{4}$$

where $\chi(x) = 1$ if $x < 0$ and is 0 otherwise. $\mu(R)$ is the chemical potential, which takes value between the Nth and $(N+1)$th eigenvalues of H to control the number of electrons. Here we assume there is a positive gap between the Nth eigenvalue and the $N+1$th eigenvalue corresponding to the Hamiltonian $H(R)$.

Since all the quantities depend on the atomic positions R, to simplify the notation we drop the dependence on R unless otherwise specified. If we approximate the eigenfunctions $\{\psi_i\}_{i=1}^N$ by linear combination of a set of basis functions $\Phi = (\phi_1,\ldots,\phi_{N_b})$, the Hamiltonian operator H is discretized into a finite dimensional matrix $\Phi^{\mathrm{T}}H\Phi$ (here and in the following, we will use the linear algebra notation: $\phi_i^{\mathrm{T}}H\phi_j = \langle\phi_i|H|\phi_j\rangle$). The number of basis functions N_b is therefore called the *discretization cost*. The electron energy and the force can be expressed in terms of the discretized Hamiltonian operator as

$$\begin{aligned} &E_\Phi = \mathrm{Tr}\big[g_0(\Phi^{\mathrm{T}}H\Phi)\big], \\ &F_{\Phi,I} = -\frac{\partial E_\Phi}{\partial R_I} = -\mathrm{Tr}\left[g_0'\big(\Phi^{\mathrm{T}}H\Phi\big)\Phi^{\mathrm{T}}\frac{\partial H}{\partial R_I}\Phi\right] - 2\mathrm{Tr}\left[g_0'\big(\Phi^{\mathrm{T}}H\Phi\big)\Phi^{\mathrm{T}}H\frac{\partial \Phi}{\partial R_I}\right]. \end{aligned} \tag{5}$$

$F_{\Phi,I}$ is the Ith component of the force. In what follows the second equation in (5) is also written in a compact form as

$$F_\Phi = -\frac{\partial E_\Phi}{\partial R} = -\mathrm{Tr}\left[g_0'\big(\Phi^{\mathrm{Tr}}H\Phi\big)\Phi^{\mathrm{Tr}}\frac{\partial H}{\partial R}\Phi\right] - 2\mathrm{Tr}\left[g_0'\big(\Phi^{\mathrm{Tr}}H\Phi\big)\Phi^{\mathrm{Tr}}H\frac{\partial \Phi}{\partial R}\right]. \tag{6}$$

Choosing basis functions Φ adaptively with respect to the atomic positions R has obvious computational advantages, as it allows the possibility to reduce the discretization cost by a significant amount while maintaining the accuracy for the evaluation of the electron energy and atomic forces. Since the electron energy is defined variationally as in (2), an accurate basis set should minimize the electron energy. However, choosing the basis functions adaptively gives rise to some difficulties in the evaluation of the force (5) which requires the calculation of $\frac{\partial\Phi}{\partial R}$. In electronic structure theory, the contribution from $\frac{\partial\Phi}{\partial R}$ is referred to as the Pulay force [3]. We will henceforth adopt this terminology. The Pulay force originates from the incompleteness of the basis set, and has been found to be important to obtain the force with reliable accuracy for structure optimization or first principle molecular dynamics [3,4]. The calculation of the Pulay force can be quite expensive even if the basis functions Φ have analytical expressions, and the calculation of the Pulay force becomes almost intractable if the basis functions are defined implicitly such as in the adaptive mesh method [5–8]. We would like to systematically reduce the Pulay force so that the approximation

$$\frac{\partial E_\Phi}{\partial R} \approx \mathrm{Tr}\left[g_0'\big(\Phi^{\mathrm{T}}H\Phi\big)\Phi^{\mathrm{T}}\frac{\partial H}{\partial R}\Phi\right] \tag{7}$$

becomes adequate.

The key observation in this paper is that minimizing the electron energy and reducing the Pulay force can be simultaneously achieved by the following optimization procedure

$$\min_{\Phi\subset\mathcal{V},\Phi^{\mathrm{T}}\Phi=I} E_\Phi = \min_{\Phi\subset\mathcal{V},\Phi^{\mathrm{T}}\Phi=I} \mathrm{Tr}\big[g_0(\Phi^{\mathrm{T}}H\Phi)\big]. \tag{8}$$

Here $\mathcal{V}$ is an admissible subset of the space spanned by a set of *primitive basis functions* which are independent of R. Later $\mathcal{V}$ will be referred to as the *admissible set*. We select from $\mathcal{V}$ a small number of R-dependent *optimized basis functions* $\Phi = (\Phi_1,\ldots,\Phi_{N_b})$ which give rise to the lowest electron energy in $\mathcal{V}$. The Euler–Lagrange equation for the minimization problem (8) reads

$$\begin{cases} H\Phi g_0'(\Phi^{\mathrm{T}}H\Phi) = \Phi\Lambda, \\ \Phi^{\mathrm{T}}\Phi = I, \end{cases} \tag{9}$$

where the matrix Λ is a Lagrangian multiplier and is symmetric. When the first optimality condition (9) is satisfied, we find

$$2\mathrm{Tr}\left[g_0'(\Phi^{\mathrm{T}}H\Phi)\Phi^{\mathrm{T}}H\frac{\partial\Phi}{\partial R}\right] = 2\mathrm{Tr}\left[\Lambda\Phi^{\mathrm{T}}\frac{\partial\Phi}{\partial R}\right] = \mathrm{Tr}\left[\Lambda\frac{\partial(\Phi^{\mathrm{T}}\Phi)}{\partial R}\right] = 0. \tag{10}$$

The last equality comes from the orthonormal constraint on the optimized basis functions Φ. The reason why (10) holds can be understood from the variational structure of the original problem (8), which is related to the Hellmann–Feynman theorem in quantum mechanics. As a result, the Pulay force vanishes in the atomic force even if the optimized basis functions are far from being a complete basis set.

The choice of the primitive basis functions is crucial. Although the optimized basis functions are always incomplete due to the small number of basis functions used, the primitive basis set should be systematically improvable towards a complete basis set. Each primitive basis function should be local in order to be suitable for large scale parallel calculation. In our previous work [9], the primitive basis set is constructed using a discontinuous Galerkin (DG) framework. The DG primitive basis set allows the usage of basis functions that are discontinuous across element surfaces. Each DG primitive basis function is local in the real space, and thus gives full flexibility in the choice of the optimized basis functions. The locality constraint in the real space can therefore be naturally applied to the optimized basis functions, giving rise to the *optimized local basis set*.

We remark that a large primitive basis set also presents practical difficulties for the optimization procedure. In this paper we propose a preconditioned Newton–GMRES method to obtain the optimized local basis functions. Numerical results using a one dimensional model problem validate the performance of the optimized local basis functions: the electron energy and the force can be accurately calculated along the trajectory of the molecular dynamics without systematic drift, using a very small number of basis functions per atom.

Improving the quality of the basis functions via variational optimization has been previously studied in the electronic structure theory. However, to the best of our knowledge all the optimized basis functions presented so far use atom-centered primitive basis functions, such as atomic orbitals or Gaussian-type orbitals. Since atomic orbitals or Gaussian-type orbitals depend on the atomic positions and do not form a complete basis set, the Pulay force never vanishes. The Pulay force of all the primitive basis functions should be computed for each atomic configuration. Moreover, optimization for each atomic configuration is generally considered to be an expensive procedure, and the optimized basis functions are usually obtained for specific reference systems instead. For example, Junquera et al. [10] proposed to optimize the shape and cutoff radii of a set of numerical atomic orbitals; Ozaki [11] proposed using the optimal linear combination of a set of numerical atomic orbitals; Blum et al. [12] used a greedy method to select basis functions from a large pool of numerical atomic orbitals. The drawback of this procedure is that the quality of the basis functions depends heavily on the choice of the reference system. The transferability of these basis sets obtained for specific reference systems should be tested carefully for a variety of systems. Optimized basis functions without the choice of reference systems have also been studied before. Talman [13] proposed to optimize a set of numerical atomic orbitals for all the atoms simultaneously. Rayson and Briddon [14] tried to find the optimal linear combination of Gaussian-type orbitals, where the optimization process loops over each atom in the system. These methods share similar spirit as the present work, and can be regarded as approximate strategies towards achieving optimality in practice.

Our current work avoids the subtle issue of transferability by means of an optimization procedure for any given system, which could be advantageous for complex systems where manually constructed transferable basis functions are difficult to be obtained. The DG primitive basis set is a complete basis set, and the optimized local basis functions are local by construction. The DG primitive basis set is independent of the atomic positions, and the Pulay force vanishes when the optimality condition is reached.

The rest of the paper is organized as follows. In Section 2, we introduce the optimized local basis set for KSDFT. Numerical examples are presented in Section 3, followed by discussion and conclusion in Section 4. To make the paper self-contained, we briefly recall the finite temperature Kohn–Sham density functional theory in Appendix A.

2. Optimized local basis function

As introduced in our previous work [9], using a discontinuous Galerkin method (the interior penalty method [15,16]), the effective energy functional in Kohn–Sham density functional theory is given by

$$\begin{aligned}\mathcal{F}_{\mathrm{DG}}(\{\psi_i\},\{f_i\}) = {} & \frac{1}{2}\sum_i f_i\langle\nabla\psi_i,\nabla\psi_i\rangle_{\mathcal{T}} - \sum_i f_i\langle\{\{\nabla\psi_i\}\},[\![\psi_i]\!]\rangle_{\mathcal{S}} + \langle V_{\mathrm{eff}},\rho\rangle_{\mathcal{T}} + \alpha\sum_i f_i\langle[\![\psi_i]\!],[\![\psi_i]\!]\rangle_{\mathcal{S}} + \sum_\ell \gamma_\ell\sum_i f_i|\langle b_\ell,\psi_i\rangle_{\mathcal{T}}|^2 \\ & + \beta^{-1}\sum_i (f_i\ln f_i + (1-f_i)\ln(1-f_i)).\end{aligned} \tag{11}$$

This is a discretization method for the Helmholtz free energy (A.18) for a system at temperature β^{-1}, see Appendix A for details of formulation of Kohn–Sham density functional theory in finite temperature. Here $\mathcal{T}$ is a collection of quasi-uniform rectangular partitions of the computational domain:

$$\mathcal{T} = \{E_1, E_2, \ldots, E_M\}, \tag{12}$$

and $\mathcal{S}$ be the collection of surfaces that correspond to $\mathcal{T}$. $\langle\cdot,\cdot\rangle_{\mathcal{T}}$ and $\langle\cdot,\cdot\rangle_{\mathcal{S}}$ are inner products in the bulk and on the surface respectively. The notations $\{\{\cdot\}\}$ and $[\![\cdot]\!]$ are used for the standard average and jump operators across surfaces in the interior penalty method. We refer to [9] for more details.

Let Φ be a chosen set of basis functions $\Phi = \{\varphi_{k,j}\}_{j=1}^{J_k}$, where each $\varphi_{k,j}$ is supported in E_k and J_k is the total number of basis functions in E_k. The corresponding approximation space $\mathcal{V}_\Phi$ is given by

$$\mathcal{V}_\Phi = \mathrm{span}\{\varphi_{k,j}, E_k \in \mathcal{T}, \quad j = 1,\ldots,J_k\}. \tag{13}$$

The approximated Kohn–Sham orbitals are the solutions to the minimization problem

$$\begin{aligned} &\min_{\{\psi_i\}\subset\mathcal{V}_\Phi,\{f_i\}} \mathcal{F}_{\mathrm{DG}}(\{\psi_i\},\{f_i\}),\\ &\text{s.t.} \quad \int \psi_i^*\psi_j \mathrm{d}x = \delta_{ij}, \quad i,j = 1,\ldots,\widetilde{N}, \end{aligned} \tag{14}$$

where $\widetilde{N}$ is chosen to be slightly larger than the number of electrons N in the system in order to compensate for the finite temperature effect (see Appendix A for more detailed explanation). We propose the optimized local basis functions which give rise to a specific choice of Φ, in order to achieve accuracy for both the Helmholtz free energy and the force while using a small number of basis functions. Following the spirit of (8) introduced for the model problem in the introduction, the optimized local basis function set Φ solves the following minimization problem

$$\min_{\Phi\subset\mathcal{V},\Phi^T\Phi=I} \min_{\{\psi_i\}\subset\mathcal{V}_\Phi,\{f_i\}} \mathcal{F}_{\mathrm{DG}}(\{\psi_i\},\{f_i\}), \tag{15}$$

where $\mathcal{V}$ is the *admissible set*. To define the admissible set, we take for each element E_k a set of basis functions $\{u_{k,j}, j = 1,\ldots J_k\}$. Each $u_{k,j}$ is compactly supported in E_k, and they satisfy the orthonormality condition

$$\langle u_{k',j'}, u_{k,j}\rangle_{\mathcal{T}} = \delta_{kk'}\delta_{jj'}. \tag{16}$$

For example, $\{u_{k,j}\}$ can be polynomials restricted to the set E_k up to a certain order. Other forms of primitive basis functions can be chosen as well, without changing the discussion that follows. The discretized Hamiltonian in the DG formulation takes the form

$$\begin{aligned} H_{k'j';kj} = &\frac{1}{2}\langle\nabla u_{k'j'}, \nabla u_{kj}\rangle_{\mathcal{T}} - \frac{1}{2}\langle[\![u_{k'j'}]\!], \{\{\nabla u_{kj}\}\}\rangle_{\mathcal{S}} - \frac{1}{2}\langle\{\{\nabla u_{k'j'}\}\}, [\![u_{kj}]\!]\rangle_{\mathcal{S}} + \alpha\langle[\![u_{k'j'}]\!], [\![u_{kj}]\!]\rangle_{\mathcal{S}} + \langle u_{k'j'}, V_{\mathrm{eff}}u_{kj}\rangle_{\mathcal{T}}\\ &+ \sum_\ell \gamma_\ell \langle u_{k'j'}, b_\ell\rangle_{\mathcal{T}}\langle b_\ell, u_{kj}\rangle_{\mathcal{T}}. \end{aligned} \tag{17}$$

The optimized local basis functions should be local in the real space in order to facilitate large scale computation. Since $\{u_{k,j}\}$ are compactly supported in E_k, the locality constraint on the optimized local basis functions is naturally imposed by requiring each function in the admissible set to be linear combinations of $\{u_{k,j}\}$ for the same k, *i.e.*

$$\mathcal{V} = \bigcup_{k=1}^{M} \mathrm{span}\{u_{k,j}, \quad j = 1,\ldots,J_k\}, \tag{18}$$

where M is the number of elements.

Inside each element E_k, we select N_k optimized local basis functions from the admissible set. N_k is much smaller than J_k. The optimized local basis functions are denoted by $\{\Phi_{k,1},\ldots,\Phi_{k,N_k}\}$, and are represented by the linear combination of the primitive basis functions

$$\Phi_{k,l} = \sum_{j=1}^{J_k} \tilde{\Phi}_{k,l,j}u_{k,j}, \quad l = 1,\ldots,N_k.$$

With slight abuse of notation, we use $\Phi_{k,l}$ also for the column vector of the coefficients in the primitive basis functions:

$$\Phi_{k,l} = \begin{pmatrix} \tilde{\Phi}_{k,l,1} & \tilde{\Phi}_{k,l,2} & \cdots & \tilde{\Phi}_{k,l,J_k} \end{pmatrix}^{\mathrm{T}}. \tag{19}$$

If we write

$$\Phi_k = \begin{pmatrix} \Phi_{k,1} & \Phi_{k,2} & \cdots & \Phi_{k,N_k} \end{pmatrix}, \tag{20}$$

the optimized local basis set Φ represented in the primitive basis set takes the form

$$\Phi = \mathrm{diag}(\Phi_1, \Phi_2, \ldots, \Phi_M). \tag{21}$$

Because of the block diagonal structure, the orthonormality constraint $\Phi^T\Phi = I$ is equivalent to the orthonormal constraint for each Φ_k, *i.e.*, $\Phi_k^T\Phi_k = I_k$, $k = 1,\ldots,M$. Here each block Φ_i is a rectangular matrix of size $N_g \times N_k$, where N_g is the number of grid points in the element, and N_k is the number of basis functions. I_k is an $N_k \times N_k$ identity matrix.

Under the basis set Φ, the discretized Hamiltonian becomes $\Phi^{\mathrm{T}}H\Phi$ with H given by (17). The Helmholtz free energy can be written without the explicit dependence on $\{\psi_i\}$ and $\{f_i\}$:

$$\min_{\{\psi_i\}\subset\mathcal{V}_\Phi,\{f_i\}} \mathcal{F}_{\mathrm{DG}}(\{\psi_i\},\{f_i\}) = \mathrm{Trg}(\Phi^{\mathrm{T}}H\Phi) + \mu N, \tag{22}$$

where the function g, which is a finite temperature version of g_0, is defined as

$$g(x) = -\beta^{-1}\ln(1+\exp(\beta(\mu-x))). \tag{23}$$

Note that the derivative of g is the Fermi–Dirac function

$$g'(x) = (1+\exp(\beta(x-\mu)))^{-1}. \tag{24}$$

Hence, the minimization problem (15) becomes

$$\begin{aligned} &\mathcal{F}_{\mathrm{DG}} = \min_{\Phi\subset\mathcal{V}} \left[\mathrm{Trg}(\Phi^{\mathrm{T}}H\Phi) + \mu N\right], \\ &\text{s.t.} \quad \Phi_k^T\Phi_k = I_k, \quad k = 1,\ldots,M. \end{aligned} \tag{25}$$

The atomic force is then given by

$$F = -\frac{\partial \mathcal{F}_{\mathrm{DG}}}{\partial R} = -\mathrm{Tr}\left(\rho_\Phi \Phi^{\mathrm{T}}\frac{\partial H}{\partial R}\Phi\right) - 2\mathrm{Tr}\left(\rho_\Phi\Phi^{\mathrm{T}}H\frac{\partial\Phi}{\partial R}\right) = -\mathrm{Tr}\left(\rho_\Phi\Phi^{\mathrm{T}}\frac{\partial H}{\partial R}\Phi\right), \tag{26}$$

where $\rho_\Phi = g'(\Phi^{\mathrm{T}}H\Phi)$ is the single particle density matrix associated to the discretized Hamiltonian $\Phi^{\mathrm{T}}H\Phi$. ρ_Φ can be evaluated using standard diagonalization techniques by computing the eigenvalues and eigenvectors of the reduced Hamiltonian $\Phi^TH\Phi$. This is asymptotically the most time consuming step which scales as $O(N^3)$ where N is the number of electrons in the system. For the 1D system considered in this manuscript, ρ_Φ is solved by the MATLAB diagonalization subroutine *eig*. For systems of large size, the diagonalization routine can be replaced by the recently developed low order scaling selected inversion methods [17,18] to reduce the computational cost. The Pulay force vanishes in the last equality when the first order optimality of the optimization problem (25) is reached, following the same reasoning as in (10).

The Euler–Lagrange equation with respect to the minimization problem (25) reads

$$\begin{cases} H\Phi\rho_\Phi - \Phi\Lambda = 0, \\ \Phi^{\mathrm{T}}\Phi - I = 0, \end{cases} \tag{27}$$

where the Λ is a block diagonal matrix

$$\Lambda = \mathrm{diag}(\Lambda_1,\Lambda_2,\ldots,\Lambda_M),$$

which is the Lagrange multiplier for the orthonormal constraints. Due to the block diagonal structure of Φ, we can write the first order optimality condition (27) as

$$\sum_j H_{ij}\Phi_j\rho_{\Phi,ji} - \Phi_i\Lambda_i = 0, \quad i = 1,\cdots,M. \tag{28}$$

Define the remainder for the ith element as

$$R_i(\Phi,\Lambda) = \begin{pmatrix} \sum_j H_{ij}\Phi_j\rho_{\Phi,ji} - \Phi_i\Lambda_i \\ I - \Phi_i^{\mathrm{T}}\Phi_i \end{pmatrix}. \tag{29}$$

We solve $R_i(\Phi,\Lambda) = 0$ for $i = 1,2,\ldots,M$.

In order to solve the nonlinear system (27), we propose a preconditioned Newton–GMRES method as follows. Denote by J the Jacobian matrix. At the lth iteration, the Newton step solves the following linear system for the correction term

$$J^{(l)}\begin{pmatrix} \Delta\Phi^{(l)} \\ \Delta\Lambda^{(l)} \end{pmatrix} = -\begin{pmatrix} H\Phi g'(\Phi^{\mathrm{T}}H\Phi) - \Phi\Lambda \\ I - \Phi^{\mathrm{T}}\Phi \end{pmatrix}. \tag{30}$$

To make the optimization feasible in practice, we take the following approximation. We neglect the derivative of $\rho_\Phi = g'(\Phi^{\mathrm{T}}H\Phi)$ with respect to Φ in the Jacobian. The most important reason for this approximation is that the numerical evaluation of such derivative is quite expensive. In practice we find that the residue of the Euler–Lagrange equation decays fast in the first few Newton iterations, and slows down when the residue becomes small, suggesting that the derivative of ρ_Φ with respect to the basis functions can be important especially for the small residue case. Numerical results indicate that the accuracy of the Helmholtz free energy and the force can already be improved by one order of magnitude after a few Newton iterations. Further improvement that includes the approximate form of the derivative of ρ_Φ will be considered in the future work. Using this approximation, the correction equation (30) can be written explicitly as

$$\begin{pmatrix} \sum_j H_{ij}(\Delta\Phi)_j\rho_{\Phi,ji} - (\Delta\Phi)_i\Lambda_i - \Phi_i(\Delta\Lambda)_i \\ -\Phi_i^{\mathrm{T}}(\Delta\Phi)_i - (\Delta\Phi)_i^{\mathrm{T}}\Phi_i \end{pmatrix} = -R_i, \tag{31}$$

for $i = 1,2,\ldots,M$.

We solve the linear system (31) using a preconditioned GMRES method. The GMRES method [19] is a robust way for solving ill-conditioned linear equations. The preconditioner should give an approximate solution efficiently for the following equation

$$\begin{pmatrix} \sum_j H_{ij}(\Delta\Phi)_j \rho_{\Phi,ji} - (\Delta\Phi)_i \Lambda_i - \Phi_i(\Delta\Lambda)_i \\ -\Phi_i^{\mathrm{T}}(\Delta\Phi)_i - (\Delta\Phi)_i^{\mathrm{T}}\Phi_i \end{pmatrix} = -\begin{pmatrix} B_i \\ C_i \end{pmatrix} \tag{32}$$

for any right hand side $\{B_i\}$,$\{C_i\}$. To this end we first neglect the interaction between different elements:

$$\begin{pmatrix} H_{ii}(\Delta\Phi)_i \rho_{\Phi,ii} - (\Delta\Phi)_i \Lambda_i - \Phi_i(\Delta\Lambda)_i \\ -\Phi_i^{\mathrm{T}}(\Delta\Phi)_i - (\Delta\Phi)_i^{\mathrm{T}}\Phi_i \end{pmatrix} = -\begin{pmatrix} B_i \\ C_i \end{pmatrix}. \tag{33}$$

The equations of $(\Delta\Phi)_i$ for different elements become decoupled. (33) can be therefore solved independently in each element. Second, we note that there are degeneracy issues solving (33). This is because in the subspace spanned by the basis $\mathcal{V}_\Phi$, only the low-lying eigenfunctions of the discrete Hamiltonian affect the free energy much, while the eigenfunctions with large eigenvalues do not contribute much due to small occupation number. Therefore, if we change the subspace $\mathcal{V}_\Phi$ in the direction of these high energy eigenfunctions, it does not change much the energy, which causes degeneracy.

We propose the following pruning method to solve the degeneracy problem. Instead of solving (33), we restrict to the basis functions contributed to the low-lying eigenfunctions by the following procedure. Given density matrix ρ_Φ, for each element E_i, we take a singular value decomposition of the diagonal block of $\rho_{\Phi,ii}$:

$$\rho_{\Phi,ii} = U_i S_i U_i^{\mathrm{T}}, \tag{34}$$

with the singular values sorted in descending order. Then according to magnitude of the singular values, we write $U_i = (U_i^h, U_i^l)$, where the singular vectors in U_i^h correspond to high singular values above a certain threshold, and the ones in U_i^l correspond to low singular values below the threshold. The basis functions in the element can be separated into two accordingly:

$$\Phi_i^h = \Phi_i U_i^h, \quad \Phi_i^l = \Phi_i U_i^l. \tag{35}$$

We now only update the correction term corresponding to the high singular values by solving

$$\begin{pmatrix} H_{ii}(\Delta\Phi)_i^h \rho_{\Phi,ii}^h - (\Delta\Phi)_i^h \Lambda_i^h - \Phi_i^h(\Delta\Lambda)_i^h \\ -\left(\Phi_i^h\right)^{\mathrm{T}}(\Delta\Phi^h)_i - (\Delta\Phi^h)_i^{\mathrm{T}}\Phi_i^h \end{pmatrix} = -\begin{pmatrix} B_i U_i^h \\ \left(U_i^h\right)^T C_i U_i^h \end{pmatrix}, \tag{36}$$

where

$$\rho_{\Phi,ij}^h = \left(U_i^h\right)^{\mathrm{T}} \rho_{\Phi,ij} U_j^h.$$

The approximate solution of the preconditioning Eq. (32) is therefore given by

$$\Delta\Phi_i = \Delta\Phi_i^h \left(U_i^h\right)^T, \quad \Delta\Lambda_i = U_i^h \Delta\Lambda_i^h (U_i^h)^T. \tag{37}$$

As will be seen in the numerical examples in Section 3, the preconditioned Newton–GMRES method is able to obtain the optimized local basis functions efficiently with a small number of iterations.

3. Numerical result

3.1. Setup

The accuracy and efficiency of the optimized local basis functions is illustrated using a one-dimensional model problem as follows. The number of atoms in the one-dimensional model problem is denoted by N_A, the positions of electrons by x, and the positions of ions by $R = (R_1, R_2, \ldots, R_{N_A})^T$. The electronic and ionic degrees of freedom are separated by the Born–Oppenheimer approximation. The effective Kohn–Sham Hamiltonian of the electrons for a given atomic configuration R is

$$H(R) = -\frac{1}{2}\Delta + V(x;R). \tag{38}$$

The effective electron–ion interaction and electron–electron interaction is modeled by the summation of a series of Gaussian functions

$$V(x;R) = -\frac{A}{\sqrt{2\pi\sigma^2}} \sum_{l=1}^{N_A} e^{-\frac{(x-R_l)^2}{2\sigma^2}}. \tag{39}$$

A and σ characterize the height and the width of the potential well around each atom, respectively. For simplicity, the effective Hamiltonian does not depend on the electron density, and hence self-consistency iteration is not involved. The self-consistent iteration will be added in the future work. The ion-ion interaction is modeled by a harmonic potential with periodized nearest-neighbor interaction

$$V_{II}(R) = \frac{1}{2}\sum_{I=1}^{N_A-1}\omega(R_I - R_{I+1})^2 + \frac{1}{2}\omega(R_{N_A} - R_1 - L)^2, \tag{40}$$

with L being the length of the computational domain. The force on atom I is

$$F_I = -\frac{\partial \mathcal{F}_{\mathrm{DG}}(R)}{\partial R_I} - \frac{\partial V_{II}(R)}{\partial R_I}. \tag{41}$$

The finite temperature KSDFT is used here and the Helmholtz free energy for the electrons $\mathcal{F}_{\mathrm{DG}}(R)$ is given by (25). The finite temperature effect is usually negligible in insulating systems with large band gap, but becomes important for the stability in metallic systems with small or vanishing band gap.

The accuracy is measured in terms of the error of the Helmholtz free energy per atom and the error of the force. For a given atomic configuration, the Helmholtz free energy per atom and the force are calculated independently using the optimized local basis functions and the benchmark plane wave basis functions. Except for the unit of temperature which is Kelvin, atomic units are used throughout this section unless otherwise specified. In particular, the unit of energy is Hartree, the unit of force is Hartree/Bohr, and the electron mass m, electron charge e and the Planck constant $\hbar$ are set to be unity. The detailed choices of the parameters in the simulation are as follows. Except in the last example where we test for different system sizes, the number of atom is taken to be $N_A = 8$. The average distance between adjacent atoms is 10 au, and the size of each element is also set to be 10 au. The initial guess of the optimized local basis functions uses the adaptive local basis functions proposed in our previous work [9]. The adaptive local basis functions use a small buffer region outside each element. The buffer size is 5 au in the present calculation. We compare the electron energy and the forces produced by the optimized local basis functions with those obtained from a planewave calculation with kinetic energy cutoff at $E_{\mathrm{cut}} = 40$ Ry, or 20 planewaves per atom. The change of the Helmholtz free energy and the force is less than 10^{-8} au if the kinetic energy cutoff for the planewave calculation is further increased. Twenty-one Legendre–Gauss–Lobatto (LGL) grid points per element are used to discretize the optimized local basis functions as well as the adaptive local basis functions. The change of the Helmholtz free energy and the force is less than 10^{-8} au if the number of LGL integration points is further increased. Therefore the numerical integration error is negligible, and the error in the calculated Helmholtz free energy and the force faithfully represents the error due to the usage of adaptive local basis functions or optimized local basis functions. The electron temperature is 2000 K. The penalty parameter α in the DG Hamiltonian is 40. The choice of parameters for the potential energy surface is $\omega = 0.03$, $A = 5.0$, $\sigma = 4.0$.

If one electron is assigned to each atom (spin degeneracy is neglected), then the band gap at the equidistant configuration is around 14,000 K, which is much larger than the electron temperature (2000 K). In what follows this system is referred to as the insulating system. If four electrons are assigned to each atom, the band gap is is essentially zero (0.5 K). The energy levels around the Fermi surface are fractionally occupied due to the thermal effect. This system is referred to as the metallic system.

In the optimization of the local basis functions, the maximum number of Newton iterations is set to be 4, and the maximum number of iterations for the preconditioned GMRES solver for the Newton's equation is set to be 30. We find that the error for solving the linear system (31) using 30 preconditioned GMRES iterations is less than 10^{-4}. The threshold value for the significant part of the basis functions is set to be 10^{-7} to avoid degeneracy. The preconditioning step is solved by direct LU decomposition method inside each element.

3.2. Static case

We first illustrate the performance of the optimized local basis set in the static case. 20 atomic configurations are generated from equidistant configuration with small random perturbations. The accuracy of using the optimized local basis set is measured by the mean absolute value of the error (mean error) of the Helmholtz free energy per atom and the mean error of the force of a fixed atom. Besides the optimized local basis functions, the error of using the adaptive local basis functions [9] is presented as well to illustrate the effectiveness of the optimization procedure.

For the insulating system, the relative error of the force is already 0.5% with as small as 4 basis functions per atom using the optimized local basis functions (Table 1). When compared to the adaptive local basis functions with the same number of basis functions per atom, the error of the Helmholtz free energy per atom is reduced by 51 times, and the error of the force is reduced by 14 times after the optimization procedure. It is illuminating to see the difference between the adaptive local basis functions and the optimized local basis functions. Since any unitary transformation of the basis functions in each element does not change the total energy of the system, the basis functions should first be rotated according a certain criterion. Here we rotate the basis functions in an element according to the Ritz values of the Hamiltonian in the same element. Take the first element for example, the Hamiltonian operator is denoted by H_{11}, and the basis functions in the first element is denoted by Φ_1. We solve the following eigenvalue problem

$$(\Phi_1^T H_{11}\Phi_1)C_1 = C_1\Lambda_1, \tag{42}$$

Table 1
Mean error of the Helmholtz free energy per atom, the absolute error of the force of the first atom, and the relative error of the force of the first atom. This system is an insulating system with 1 electron per atom (spin neglected). Four basis functions per atom are used for both the adaptive local basis functions and the optimized local basis functions.

Method	$\Delta\mathcal{F}_{DG}$/atom	Absolute ΔF	Relative ΔF
Adaptive	5.7×10^{-5}	6.8×10^{-5}	4.5×10^{-3}
Optimized	1.1×10^{-6}	4.9×10^{-6}	3.3×10^{-4}

where Λ_1 is a diagonal matrix with values sorted in ascending order. Then we compare the rotated basis functions

$$\Phi_1 C \equiv [\varphi_1, \ldots, \varphi_J] \tag{43}$$

for adaptive and optimized local basis functions in Fig. 1. It is found that the optimized local basis functions are very close to the adaptive local basis functions, indicating that the adaptive local basis functions is already very accurate in computing the total energy of the system. The agreement between the adaptive local basis functions and the optimized local basis functions is very well for basis functions of low energy (Fig. 1 (a)), and the difference enlarges for basis functions or higher energy. This can be understood as that the adaptive local basis functions include contributions from unoccupied states with relatively high energy level, while the optimized local basis functions reduce the contribution from such unoccupied states by the optimization procedure.

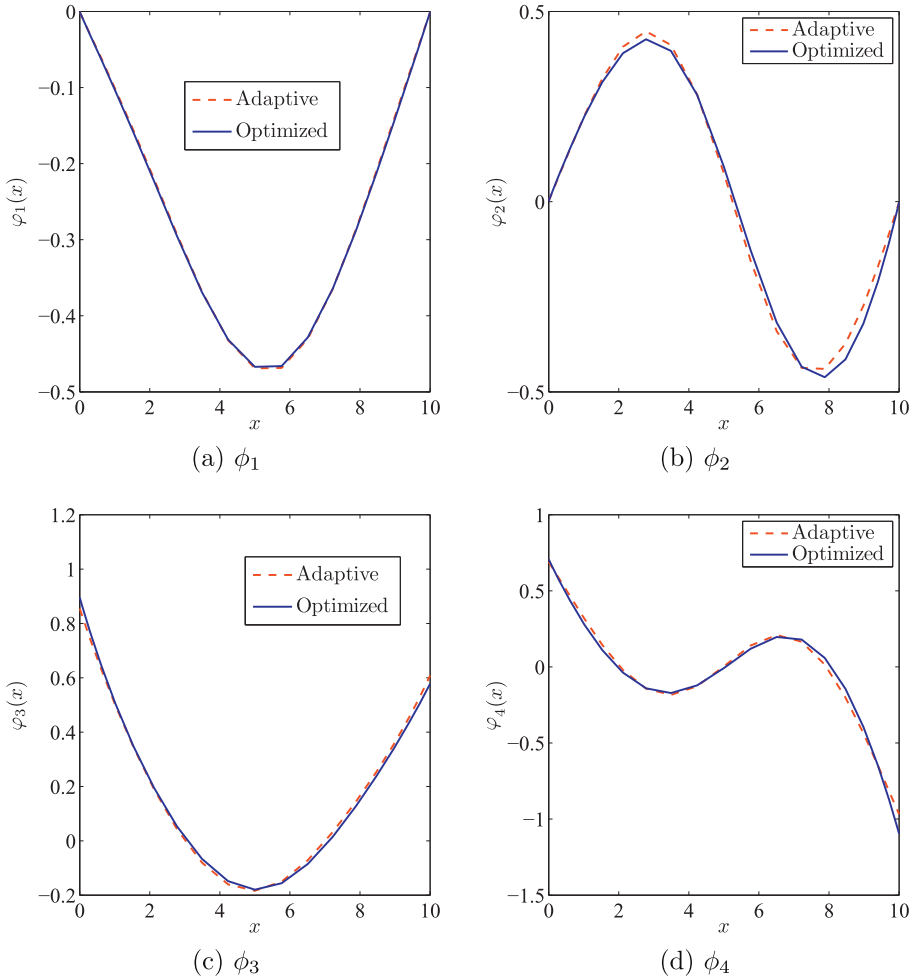

Fig. 1. Comparison of the adaptive and optimized local basis functions for an insulating system with 1 electron per atom (spin neglected). The adaptive local basis functions (red dashed line) and optimized local basis functions (blue solid line) are sorted according to the Ritz value of the local Hamiltonian in ascending order. (For interpretation of the references to colour in this figure legend, the reader is referred to the web version of this article.)

Table 2
Mean error of the Helmholtz free energy per atom, the absolute error of the force of the first atom, and the relative error of the force of the first atom. This system is a metallic system with 4 electrons per atom (spin neglected). Eight basis functions per atom are used for both the adaptive local basis functions and the optimized local basis functions.

Method	$\Delta\mathcal{F}_{DG}$/atom	Absolute ΔF	Relative ΔF
Adaptive	1.4×10^{-3}	3.8×10^{-4}	9.6×10^{-2}
Optimized	1.7×10^{-4}	4.5×10^{-6}	1.6×10^{-3}

Table 3
Mean error of the Helmholtz free energy per atom, the absolute error of the force of the first atom, and the relative error of the force of the first atom. This system is a metallic system with 4 electrons per atom (spin neglected). Twelve basis functions per atom are used for both the adaptive local basis functions and the optimized local basis functions.

Method	$\Delta\mathcal{F}_{DG}$/atom	Absolute ΔF	Relative ΔF
Adaptive	3.4×10^{-5}	1.9×10^{-7}	1.1×10^{-4}
Optimized	3.4×10^{-5}	1.7×10^{-7}	1.0×10^{-4}

Table 4
Mean error of the Helmholtz free energy per atom, the absolute error of the force of the first atom, and the relative error of the force of the first atom for a metallic system with a defect. Eight basis functions per atom are used for both the adaptive local basis functions and the optimized local basis functions.

Method	$\Delta\mathcal{F}_{DG}$/atom	Absolute ΔF	Relative ΔF
Adaptive	1.3×10^{-3}	1.1×10^{-4}	6.3×10^{-2}
Optimized	1.8×10^{-4}	5.3×10^{-6}	3.3×10^{-3}

Similar results are found for metallic systems (Table 2). More basis functions are needed in this case since there are more electrons in the metallic system than those in the insulating system studied here. The relative error of the force is 0.2% with 8 basis functions per atom using the optimized local basis functions. When compared to the adaptive local basis functions using the same number of basis functions, the error of the Helmholtz free energy per atom is reduced by 10 times and the error of the force is reduced by 60 times using the optimized local basis functions. The optimized local basis functions therefore greatly improve the accuracy with the same number of basis functions.

On the other hand, the accuracy of using the adaptive local basis functions can be systematically improved by increasing the number of basis functions per atom. For example, if the number of basis functions per atom is increased from 8 to 12 for the metallic system, the accuracy of using the adaptive local basis functions is comparable to that of using the optimized local basis functions (Table 3). This finding is fully consistent with the previous work [9] that the adaptive local basis functions also form an accurate and efficient local basis set for the electronic structure calculation. The mild increase of the number of basis functions indicates that the adaptive local basis functions are already very efficient at least for 1D or quasi-1D systems. It is also found in the previous work that the number of adaptive local basis functions increases considerably from quasi-1D systems to 3D bulk systems [9]. We expect that the number of basis functions can be reduced by a significant amount using optimized local basis functions in 3D bulk systems.

We also test the optimized local basis functions on a system with local defects. The defect system is obtained by choosing the parameter a at one atom in the potential (39) to be different from the parameters a of the rest of the atoms. The system contains eight atoms with four electrons and eight basis functions per atom. The parameter a is set to be 5.0 for all atoms except for the first atom which is set to be 3.0. The error of the Helmholtz free energy per atom and the error in the force of the defect atom are comparable to those in the periodic case (Table 4).

Finally, we compare the performance of the adaptive local basis functions and the optimized local basis functions for systems of increasing size with 8, 16, 32, 128, 256 atoms, respectively. The system is randomly perturbed by 0.2 au from the crystalline configuration, with a defect introduced at one atom of the potential. The computational time for constructing the adaptive local basis functions (red dashed line with star) and for constructing the optimized local basis functions (blue solid line with triangle) are compared in Fig. 2 (a) plotted in logarithmic scale. Five Newton steps and 30 GMRES iterations are used for the outer iteration and the inner iteration respectively in the optimization procedure. Since the optimized local basis functions use the adaptive local basis functions as an initial guess, the computational time for the optimized local basis functions also includes that for the adaptive local basis functions. The computational time for constructing both the adaptive local basis functions and the optimized local basis functions are linear thanks to the locality of the basis functions. The construction of the optimized local basis functions is 6–9 times more expensive than the construction of the adaptive local basis functions, indicating that the optimization procedure should be further improved in order to generate a practically efficient

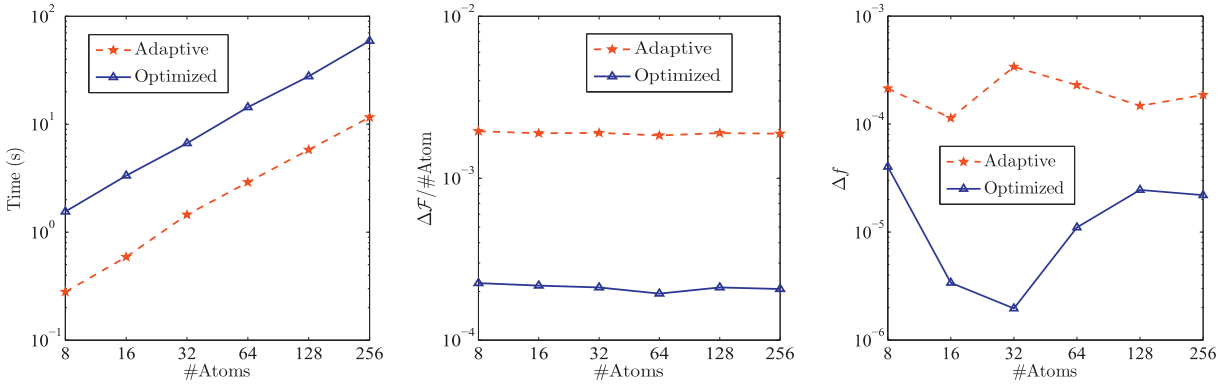

(a) Computational time (b) Error of the Helmholtz free energy per atom (c) Error of the force

Fig. 2. (a) The computational time for solving systems of various sizes using adaptive local basis functions (red dashed line) and optimized local basis functions (blue solid line). (b) The error of the Helmholtz free energy per atom using adaptive local basis functions (red dashed line) and optimized local basis functions (blue solid line). (c) The absolute error of the force for the first atom using adaptive local basis functions (red dashed line) and optimized local basis functions (blue solid line). (For interpretation of the references to colour in this figure legend, the reader is referred to the web version of this article.)

optimized local basis set. The error of the Helmholtz free energy per atom and the error of the force on the first atom are shown in Fig. 2 (b) and (c), respectively. It is found that the Helmholtz free energy obtained by the optimized local basis functions is stably 8–9 times more accurate than that obtained by the adaptive local basis functions. The ratio of improvement of the force has a much larger dependence on the realization of the atomic configuration which ranges from 5 to 170 times, with the average ratio of improvement being around one order of magnitude.

3.3. Dynamic case

The optimized local basis set is able to accurately compute the electron energy and the force using a small number of basis functions. Now we show that the optimized local basis functions can also be used in molecular dynamics. We illustrate the performance of the optimized local basis functions for molecular dynamics using the same metallic system as in Section 3.2 with four electrons and eight basis functions per atom.

In the Born–Oppenheimer approximation, the equations of motion for atom I are given by

$$M_I \ddot{R}_I = F_I, \quad I = 1, \ldots, N_A. \tag{44}$$

The mass of the ions M_I is set to be 42,000 which is close the mass of sodium in the atomic unit. F_I is the Hellman–Feynman force in (41) for atom I. The equations of motion (44) conserve the total energy given by

$$E_{IC} = \sum_{I=1}^{N_A} \frac{M_I \dot{R}_I^2}{2} + \mathcal{F}_{\mathrm{DG}}(R) + V_{II}(R). \tag{45}$$

The numerical conservation of the total energy is quantified by the drift of E_{IC}, which is defined as the relative difference of E_{IC} along the trajectory, *i.e.*

$$\mathrm{Drift}(t) = \frac{|E_{IC}(t) - E_{IC}(0)|}{|E_{IC}(0)|}. \tag{46}$$

Velocity–Verlet scheme [20] is used to propagate the equations of motion for the atoms with the time step Δt = 1.21 femtoseconds (fs). The simulation length is 10,000 steps and the total length of the simulation is 12.1 picoseconds (ps). To ensure the time-reversibility of the numerical scheme, the optimized local basis functions use the adaptive local basis functions as the initial guess at every time step. However, this is not a necessary requirement and can be improved by other time-reversible schemes such as the extended Lagrangian Born–Oppenheimer method [21]. The initial configurations of the atoms are perturbed by 0.2 au away from the equilibrium equidistant configuration, and the initial kinetic energy of the atoms is 1000 K with the mean velocity of all atoms (*i.e.* the velocity of the centroid) being zero. The error of the force and the error of the Helmholtz free energy per atom are well within 2.5×10^{-6} and 1.4×10^{-4}, respectively (see Fig. 3 (a) and (b)), which is consistent with the behavior of errors in the static calculation. The Helmholtz free energy obtained from the optimized local basis functions is systematically higher than that in the benchmark planewave simulation. The sources of the systematic shift are the penalty parameter α in the DG formulation, and that the minimization procedure is restricted to an admissible

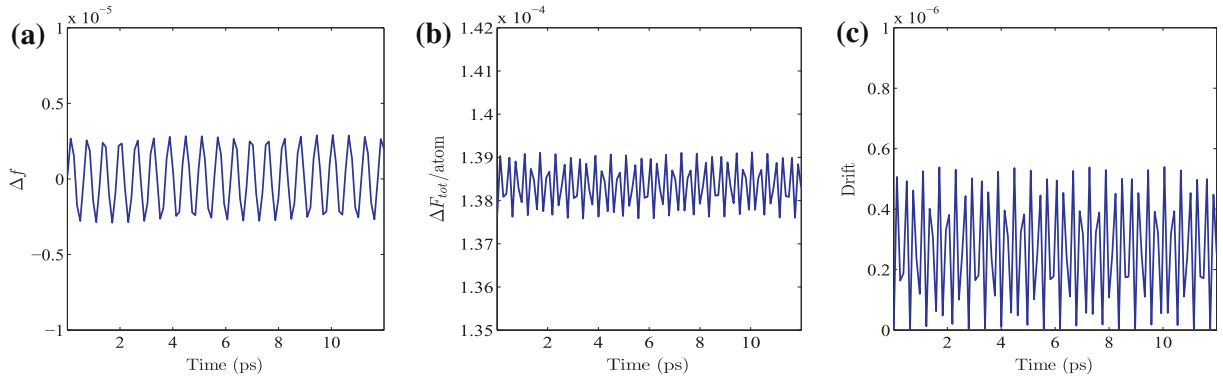

Fig. 3. The error of the force of the first atom (a), the error of the Helmholtz free energy per atom (b) and the drift of the conserved quantity (c) along the trajectory of the MD simulation plotted every 0.12 ps. The system is metallic with four electrons and eight basis functions per atom. The mean deviation of the force is unbiased.

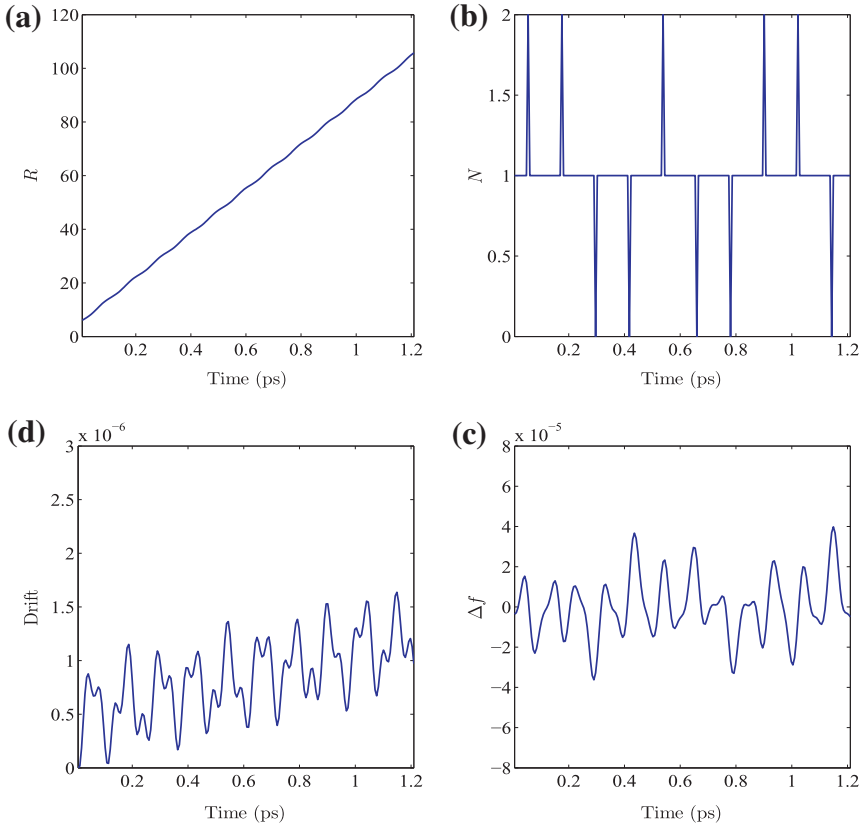

Fig. 4. The trajectory of the first atom (a), the number of atoms in the first element (b), the drift of the conserved quantity (c), and the error of the force of the first atom (d) along the trajectory of the MD simulation plotted every 0.006 ps. The system is metallic with four electrons. Eight basis functions are used per atom. The initial velocity of the centroid of mass is chosen to be 0.016 au, and hence the atoms keep crossing the boundary of the elements during the simulation.

set of the space spanned by the primitive functions. Nonetheless, the mean deviation of the force is unbiased, indicating that the structure of the trajectory obtained using the optimized local basis functions is well preserved. The drift of the conserved quantity (46) is also well controlled within 5×10^{-7} (Fig. 3 (c)).

Finally, we demonstrate that although the basis functions are discontinuous at the boundary of the elements, such discontinuity does not deteriorate the accuracy even in the case when atoms cross the boundary. To this end we assign the velocity of the centroid of mass to be 0.016 au, which is large enough so that atoms keep crossing the boundary of elements.

The system is metallic with four electrons. Eight basis functions are used per atom. The time duration of the simulation is 1.21 ps, and the length of the whole domain is 80 au. Fig. 4 (a) shows the trajectory of the first atom, which has crossed the whole domain in the simulation (note the periodic boundary condition imposed). The number of atoms in the first element is also fluctuating between 0 and 2 during the simulation, as shown in Fig. 4 (b). The drift of the conserved quantity as in Fig. 4 (c) is well controlled during the simulation. Mild deviation of the conserved quantity is observed, but we expect that such small deviation will not lead to observable effects during the molecular dynamics simulation, especially in the canonical ensemble simulation with fixed temperature. Furthermore, Fig. 4 (d) shows that the error of the force is also controlled within 4×10^{-5} au and is smooth during the simulation.

4. Conclusion

We have developed the optimized local basis set to solve models in the Kohn–Sham density functional theory for both insulating and metallic systems. The optimized local basis functions form an accurate basis set for computing the electron energy as well as the atomic force with a small number of basis functions per atom. When the optimality condition is achieved, the optimized local basis functions give the lowest energy among all the basis functions in an admissible set determined by the primitive basis functions. The force is accurately described by the Hellmann–Feynman force, and the contribution of the derivative of the basis functions (*i.e.* the Pulay force) vanishes automatically. The concept of the optimized local basis functions is quite general, and the methods developed in this paper are useful for other problems such as selecting basis functions and evaluating parameter-dependent functions as well.

To obtain the optimized local basis functions in practice, we proposed a preconditioned Newton–GMRES method. The resulting optimized local basis functions are tested using a one-dimensional model problem. We find that the optimized local basis functions accurately compute the Helmholtz free energy and the force using a very small number of basis functions per atom for both insulating and metallic systems. When applied to the molecular dynamics simulation, the optimized local basis functions do not exhibit any systematic drift in terms of the force or the total energy for the ionic degrees of freedom. Therefore the optimized local basis functions are able to give the correct statistical and dynamical properties along the molecular dynamics trajectory, and can be used for long time molecular dynamics simulation.

The optimized local basis set provides an implementable criterion to eliminate the artificial effect in the force due to the change of the basis functions and to maintain a small set of basis functions, which makes the optimized local basis set an ideal tool in the molecular dynamics simulation. However, the construction of the optimized local basis functions is found to be already more expensive than other choices such as adaptive local basis functions, indicating that the optimization procedure should be further improved especially when applied to Kohn–Sham density functional theory in 3D. The more efficient scheme may be achieved by including a feasible approximation of the derivative of the density matrix with respect to the basis function, a more efficient preconditioner for the GMRES iteration, or even a more efficient gradient method instead of a Newton-type method. These will be our future work.

Acknowledgments

W.E. and L.L. are partially supported by DOE under Contract No. DE-FG02–03ER25587 and by NSF under Contract No. DMS-0914336. L.Y. is partially supported by an Alfred P. Sloan Research Fellowship and an NSF CAREER award DMS-0846501. The authors thank the hospitality of Shanghai Jiao Tong University where part of the work was done.

Appendix A. Finite temperature Kohn–Sham density functional theory

In this appendix, we briefly described the basic formulation of the Kohn–Sham density functional theory [1,2] and its finite temperature generalization. In the Kohn–Sham density functional theory, the ground state electron energy is written as

$$E_{\rm tot} = E_{\rm tot}(\{\psi_i\}) = \frac{1}{2}\sum_{i=1}^{N}\int |\nabla\psi_i|^2 {\rm d}x + \int V_{\rm ext}\rho {\rm d}x + \sum_{\ell}\gamma_\ell \sum_{i=1}^{N}\left|\int b_\ell^*\psi_i {\rm d}x\right|^2 + \frac{1}{2}\int\int \frac{\rho(x)\rho(y)}{|x-y|}{\rm d}x{\rm d}y + \int \epsilon_{\rm xc}[\rho(x)]{\rm d}x, \tag{A.1}$$

where the Kohn–Sham orbitals are the solutions to the minimization problem

$$\begin{aligned} &\min_{\{\psi_i\}_{i=1}^N} E_{\rm tot}(\{\psi_i\}),\\ &\text{s.t.} \quad \int \psi_i^*\psi_j {\rm d}x = \delta_{ij}, \quad i,j = 1,\ldots,N. \end{aligned} \tag{A.2}$$

With slight abuse of the notation, we denote by $\{\psi_i\}$ both the arguments in the minimization problem (A.2), and the solutions to the minimization problem, *i.e.* the Kohn–Sham orbitals. The electron density is $\rho(x) = \sum_{i=1}^N |\psi_i(x)|^2$. We have neglected the spin degeneracy. The first term of (A.1) is the kinetic energy. The second and third terms come from pseudopotential, which we have taken the Kleinman–Bylander form [22]. The pseudopotential is given by

$$V_{\rm PS} = V_{\rm ext} + \sum_{\ell}\gamma_\ell |b_\ell\rangle\langle b_\ell|.$$

For each ℓ, b_ℓ is a function supported locally in the real space around the position of one of the atoms, $\gamma_\ell = +1$ or -1, and we have used the Dirac bra-ket notation. The fourth term is the Coulomb interaction between electrons, and the fifth term is the exchange–correlation functional, for which the local density approximation (LDA) [23,24] is adopted. The proposed method can also be used for more complicated exchange–correlation functionals such as the generalized gradient approximation (GGA) functionals [25].

The ground state electron energy defined in (A.1) is applicable to insulating systems with large band gap, but is difficult to evaluate for zero-gap metallic systems. For metallic system, finite temperature KSDFT becomes the standard tool [26], in which the Helmholtz free energy is considered instead. For given finite temperature $T > 0$, the Helmholtz free energy is given by

$$\begin{aligned}\mathcal{F}_{\mathrm{tot}} &= \mathcal{F}_{\mathrm{tot}}(\{\psi_i\},\{f_i\}) \\ &= \frac{1}{2}\sum_i f_i \int |\nabla\psi_i|^2 \mathrm{d}x + \int V_{\mathrm{ext}}\rho \mathrm{d}x + \sum_\ell \gamma_\ell \sum_i f_i \left|\int b_\ell^* \psi_i \mathrm{d}x\right|^2 + \frac{1}{2}\int\int \frac{\rho(x)\rho(y)}{|x-y|}\mathrm{d}x\mathrm{d}y + \int \epsilon_{\mathrm{xc}}[\rho(x)]\mathrm{d}x \\ &\quad + \beta^{-1}\sum_i (f_i \ln f_i + (1-f_i)\ln(1-f_i)).\end{aligned} \tag{A.3}$$

Correspondingly $\{\psi_i\}$ and $\{f_i\}$ are the solutions to the minimization problem

$$\begin{aligned}&\min_{\{\psi_i\},\{f_i\}} \mathcal{F}_{\mathrm{tot}}(\{\psi_i\},\{f_i\}), \\ &\text{s.t.} \quad \int \psi_i^* \psi_j \mathrm{d}x = \delta_{ij}, \quad i,j = 1,\ldots,\widetilde{N}.\end{aligned} \tag{A.4}$$

Here β is the inverse temperature $\beta = 1/k_B T$. The number of eigenstates $\widetilde{N}$ is chosen to be slightly larger than the number of electrons N in order to compensate for the finite temperature effect, following the criterion that the occupation number $f_{\widetilde{N}}$ is sufficiently small (less than 10^{-8}). $\{f_i\} \in [0,1]$ are the occupation numbers which add up to the total number of electrons $N = \sum_{i=1}^{N} f_i$, and the electron density $\rho = \sum_{i=1}^{N} f_i |\psi_i|^2$. Compared to (A.1), the only extra term is the last term, which characterizes the entropic contribution.

The Kohn–Sham equation, or the Euler–Lagrange equation associated with (A.4) reads

$$H[\rho]\psi_i = \left(-\frac{1}{2}\Delta + V_{\mathrm{eff}}[\rho] + \sum_\ell \gamma_\ell |b_\ell\rangle\langle b_\ell|\right)\psi_i = \lambda_i \psi_i, \tag{A.5}$$

where the effective one-body potential V_{eff} is given by

$$V_{\mathrm{eff}}[\rho](x) = V_{\mathrm{ext}}(x) + \int \frac{\rho(y)}{|x-y|}\mathrm{d}y + \epsilon'_{\mathrm{xc}}[\rho(x)]. \tag{A.6}$$

The occupation numbers are given by

$$f_i = \frac{1}{1+\exp(\beta(\lambda_i - \mu))}, \tag{A.7}$$

which is the Fermi–Dirac distribution evaluated at λ_i. Here μ is the chemical potential, which is chosen so that f_i satisfies

$$\sum_i f_i = N. \tag{A.8}$$

Note that (A.5) is a nonlinear eigenvalue problem, as V_{eff} depends on ρ, which is in turn determined by $\{\psi_i\}$. The electron density is self-consistent if both (A.5) and (A.6) are satisfied. After obtaining the self-consistent electron density, the Helmholtz free energy can be expressed as

$$\begin{aligned}\mathcal{F}_{\mathrm{tot}} &= \mathcal{F}_{\mathrm{tot}}(\rho,\mu) \\ &= \sum_i f_i\lambda_i + \beta^{-1}\sum_i (f_i \ln f_i + (1-f_i)\ln(1-f_i)) - \frac{1}{2}\int\int \frac{\rho(x)\rho(y)}{|x-y|}\mathrm{d}x\mathrm{d}y + \int \epsilon_{\mathrm{xc}}[\rho(x)]\mathrm{d}x - \int \epsilon'_{\mathrm{xc}}[\rho(x)]\rho(x)\mathrm{d}x.\end{aligned} \tag{A.9}$$

The goal of finite temperature Kohn–Sham density functional theory is to calculate the free energy $\mathcal{F}_{\mathrm{tot}}$, the self-consistent electron density ρ and also the chemical potential μ given the number of electrons, the temperature and the atomic configuration. The Helmholtz free energy $\mathcal{F}_{\mathrm{tot}}(R)$ plays the role of the electron energy $E(R)$ in Section 1, and the force is defined as the negative gradient of the Helmholtz free energy $F(R) = -\frac{\partial \mathcal{F}_{\mathrm{tot}}(R)}{\partial R}$. The Helmholtz free energy is applicable to both the insulating and the metallic systems. As $T \to 0$, the Helmholtz free energy $\mathcal{F}_{\mathrm{tot}}$ reduces to the ground state electron energy E_{tot}. Therefore (A.1) is also called the zero temperature KSDFT.

As f_i is given by the Fermi–Dirac distribution, we have

$$\sum_i f_i\lambda_i = \mathrm{Tr}\frac{H}{1+\exp(\beta(H-\mu))}; \tag{A.10}$$

$$\sum_i f_i \ln f_i = \mathrm{Tr}\frac{1}{1+\exp(\beta(H-\mu))}\ln\frac{1}{1+\exp(\beta(H-\mu))}; \tag{A.11}$$

$$\sum_i (1-f_i)\ln(1-f_i) = \mathrm{Tr}\frac{\exp(\beta(H-\mu))}{1+\exp(\beta(H-\mu))}\ln\frac{\exp(\beta(H-\mu))}{1+\exp(\beta(H-\mu))}. \tag{A.12}$$

Using these, we can rewrite (A.9) as (see *e.g.* [27])

$$\mathcal{F}_{\mathrm{tot}}(\rho,\mu) = -\beta^{-1}\mathrm{Tr}\ln(1+\exp(\beta(\mu-H[\rho]))) + \mu N - \frac{1}{2}\int\int\frac{\rho(x)\rho(y)}{|x-y|}\mathrm{d}x\mathrm{d}y + \int\epsilon_{\mathrm{xc}}[\rho(x)]\mathrm{d}x - \int\epsilon'_{\mathrm{xc}}[\rho(x)]\rho(x)\mathrm{d}x. \tag{A.13}$$

One can verify by straightforward calculations that

$$\frac{\delta\mathcal{F}_{\mathrm{tot}}(\rho,\mu)}{\delta\rho} = 0 \tag{A.14}$$

if ρ and μ are the self-consistent solution of the Kohn–Sham equation (A.5). Taking derivative of (A.13) with respect to μ, we have

$$\frac{\partial\mathcal{F}_{\mathrm{tot}}(\rho,\mu)}{\partial\mu} = -\mathrm{Tr}\frac{\exp(\beta(\mu-H))}{1+\exp(\beta(\mu-H))} + N = 0. \tag{A.15}$$

Therefore, the atomic force takes the form

$$F = -\frac{\mathrm{d}\mathcal{F}_{\mathrm{tot}}(\rho,\mu,R)}{\mathrm{d}R} = -\frac{\partial\mathcal{F}_{\mathrm{tot}}(\rho,\mu,R)}{\partial R} = -\mathrm{Tr}\left[\frac{1}{1+\exp(\beta(H-\mu))}\frac{\partial H}{\partial R}\right]. \tag{A.16}$$

This is known as the Hellman–Feynman theorem at finite temperature.

The Kohn–Sham density functional theory is usually solved by using the self-consistent iteration, where at each iteration, the electron density $\tilde{\rho}$ is obtained from effective Hamiltonian H_{eff}. Given an effective potential V_{eff}, and hence the effective Hamiltonian

$$H_{\mathrm{eff}} = -\frac{1}{2}\Delta + V_{\mathrm{eff}} + \sum_\ell \gamma_\ell |b_\ell\rangle\langle b_\ell|, \tag{A.17}$$

we find $\tilde{\rho}$ from $\tilde{\rho}(x) = \sum_i f_i|\psi_i(x)|^2$ where $\{\psi_i\}$'s are eigenfunctions of H_{eff}, and the definition of $\{f_i\}$ follows (A.7) and (A.8). Note that the $\{\psi_i\}$ and $\{f_i\}$'s minimize the variational problem

$$\mathcal{F}_{\mathrm{eff}}(\{\psi_i\},\{f_i\}) = \frac{1}{2}\sum_i\int f_i|\nabla\psi_i(x)|^2\mathrm{d}x + \int V_{\mathrm{eff}}(x)\rho(x)\mathrm{d}x + \sum_\ell\gamma_\ell\sum_i f_i|\langle b_\ell,\psi_i\rangle|^2 + \beta^{-1}\sum_i(f_i\ln f_i + (1-f_i)\ln(1-f_i)), \tag{A.18}$$

with the orthonormality constraints $\langle\psi_i|\psi_j\rangle = \delta_{ij}$.

References

[1] P. Hohenberg, W. Kohn, Inhomogeneous electron gas, Phys. Rev. 136 (1964) B864–B871.
[2] W. Kohn, L. Sham, Self-consistent equations including exchange and correlation effects, Phys. Rev. 140 (1965) A1133–A1138.
[3] P. Pulay, Ab initio calculation of force constants and equilibrium geometries in polyatomic molecules I. Theory, Mol. Phys. 17 (1969) 197–204.
[4] P. Bendt, A. Zunger, Simultaneous relaxation of nuclear geometries and electric charge densities in electronic structure theories, Phys. Rev. Lett. 50 (1983) 1684–1688.
[5] E. Tsuchida, M. Tsukada, Adaptive finite-element method for electronic-structure calculations, Phys. Rev. B 54 (1996) 7602.
[6] F. Gygi, G. Galli, Real-space adaptive-coordinate electronic-structure calculations, Phys. Rev. B 52 (1995) R2229.
[7] E. Bylaska, M. Holst, J. Weare, Adaptive finite element method for solving the exact Kohn–Sham equation of density functional theory, J. Chem. Theor. Comput. 5 (2009) 937.
[8] D. Zhang, L. Shen, A. Zhou, X. Gong, Finite element method for solving Kohn–Sham equations based on self-adaptive tetrahedral mesh, Phys. Lett. A 372 (2008) 5071.
[9] L. Lin, J. Lu, L. Ying, W. E, Adaptive local basis set for Kohn–Sham density functional theory in a discontinuous Galerkin framework I: Total energy calculation, J. Comput. Phys. 231 (2012) 2140.
[10] J. Junquera, O. Paz, D. Sanchez-Portal, E. Artacho, Numerical atomic orbitals for linear-scaling calculations, Phys. Rev. B 64 (2001) 235111.
[11] T. Ozaki, Variationally optimized atomic orbitals for large-scale electronic structures, Phys. Rev. B 67 (2003) 155108.
[12] V. Blum, R. Gehrke, F. Hanke, P. Havu, V. Havu, X. Ren, K. Reuter, M. Scheffler, Ab initio molecular simulations with numeric atom-centered orbitals, Comput. Phys. Commun. 180 (2009) 2175–2196.
[13] J.D. Talman, Variationally optimized numerical orbitals for molecular calculations, Phys. Rev. Lett. 84 (2000) 855.
[14] M.J. Rayson, P.R. Briddon, Highly efficient method for Kohn–Sham density functional calculations of 500–10,000 atom systems, Phys. Rev. B 80 (2009) 205104.
[15] I. Babuška, M. Zlámal, Nonconforming elements in the finite element method with penalty, SIAM J. Numer. Anal. 10 (1973) 863–875.
[16] D.N. Arnold, An interior penalty finite element method with discontinuous elements, SIAM J. Numer. Anal. 19 (1982) 742–760.

[17] L. Lin, J. Lu, L. Ying, W. E, Pole-based approximation of the Fermi–Dirac function, Chinese Ann. Math. 30B (2009) 729.
[18] L. Lin, C. Yang, J. Meza, J. Lu, L. Ying, W. E, SelInv – an algorithm for selected inversion of a sparse symmetric matrix, ACM. Trans. Math. Software 37 (2010) 40.
[19] Y. Saad, M. Schultz, GMRES: a generalized minimal residual algorithm for solving nonsymmetric linear systems, SIAM J. Sci. Stat. Comput. 7 (1986) 856.
[20] D. Frenkel, B. Smit, Understanding Molecular Simulation: From Algorithms to Applications, Academic Press, 2002.
[21] A. Niklasson, Extended Born–Oppenheimer molecular dynamics, Phys. Rev. Lett. 100 (2008) 123004.
[22] L. Kleinman, D. Bylander, Efficacious form for model pseudopotentials, Phys. Rev. Lett. 48 (1982) 1425–1428.
[23] D. Ceperley, B. Alder, Ground state of the electron gas by a stochastic method, Phys. Rev. Lett. 45 (1980) 566–569.
[24] J. Perdew, A. Zunger, Self-interaction correction to density-functional approximations for many-electron systems, Phys. Rev. B 23 (1981) 5048–5079.
[25] J. Perdew, K. Burke, M. Ernzerhof, Generalized gradient approximation made simple, Phys. Rev. Lett. 77 (1996) 3865.
[26] N. Mermin, Thermal properties of the inhomogeneous electron gas, Phys. Rev. 137 (1965) A1441–A1443.
[27] A. Alavi, J. Kohanoff, M. Parrinello, D. Frenkel, Ab initio molecular dynamics with excited electrons, Phys. Rev. Lett. 73 (1994) 2599.